A KINETIC STUDY OF THE CYTOCHROME *c*–HYDROGEN PEROXIDE REACTION

Joaquin F. PEREZ-BENITO

Departamento de Quimica Fisica, Facultad de Quimica, Universidad de Barcelona, Marti i Franques, 1, 08028 Barcelona, Spain; e-mail: jfperezdebenito@ub.edu

Received March 9, 2006
Accepted September 21, 2006

The kinetics of the reaction of cytochrome *c* with H_2O_2 was studied in aqueous phosphate media near physiological pH (5.7–7.2). The UV-VIS spectra indicated that the heme prosthetic group of the protein suffered an oxidative degradation during the reaction. The experimental rate law was $v = k_{exp}$ [cytochrome *c*] $[H_2O_2]$, with $k_{exp} = (A + B\,[H^+])/(1 + C\,[H^+])$. The apparent activation parameters associated with k_{exp} were E_a = 46 ± 2 kJ mol^{-1}, $\Delta H^{o}_{\neq}$ = 43 ± 2 kJ mol^{-1} and $\Delta S^{o}_{\neq}$ = –111 ± 5 J K^{-1} mol^{-1}. The reaction showed base catalysis and was also catalyzed by both CrO_4^{2-} and acrylamide. It was inhibited by the oxidants WO_4^{2-}, MoO_4^{2-}, VO_3^- and $[Fe(CN)_6]^{3-}$ as well as by the reductants $[Fe(CN)_6]^{4-}$ and D-mannitol, whereas Zn^{2+} and superoxide dismutase had no appreciable effect. The results are consistent with initial reduction of iron from Fe(III) to Fe(II) (supported by inhibition caused by most oxidants), followed by a hydroxyl-radical mediated oxidative degradation of the heme prosthetic group (supported by the inhibition caused by both $[Fe(CN)_6]^{4-}$ and D-mannitol).

Keywords: Cytochrome *c*; Hydrogen peroxide; Hydroxyl radicals; Kinetics; Mechanism; Proteins; Oxidative degradation; UV-VIS spectroscopy.

The free-radical theory of aging explains senescence and other degenerative diseases as caused by free radicals formed in the cells of aerobic organisms as byproducts of the oxygen metabolism. In that process, which takes place mainly in the mitochondria, oxygen molecules are partially reduced to water. The formation of free radicals can be envisaged if that reduction is schematically represented as a sequence of four consecutive, one-electron transfer reactions

$$O_2 \xrightarrow{e} O_2^{\bullet -} \xrightarrow[2\,H^+]{e} H_2O_2 \xrightarrow{e} HO^- + HO^{\bullet} \xrightarrow[2\,H^+]{e} 2\,H_2O \qquad (1)$$

involving the formation of three toxic intermediates, two free radicals (superoxide ion and hydroxyl radical) and a hydrogen peroxide molecule. Although the intracellular biochemical machinery of aerobes is designed so that the formation of those toxic intermediates is avoided as much as possi-

Collect. Czech. Chem. Commun. 2006, Vol. 71, Nos. 11–12, pp. 1588–1610

doi:10.1135/cccc20061588

ble, some of them would inevitably be formed, and the slow accumulation of chemical lesions caused by them in key cellular structures, such as DNA or membranes, would eventually lead to the process known as aging. Because of its exacerbated reactivity, the hydroxyl radical might be the most damaging chemical species for aerobic organisms under ordinary physiological conditions[1]. As shown in Eq. (*1*), the formation of hydroxyl radicals under those conditions requires the reaction of hydrogen peroxide with a one-electron donor, and transition-metal ions in their lower oxidation states are the logical candidates for that role[2]. Iron is the most abundant transition-metal element in the human body, its intracellular concentration being in most tissues in the micromolar range[3], and it is generally thought that the main biological source of hydroxyl radicals might be the Fe(II) + H_2O_2 reaction[4]. However, consensus on this crucial point is far from being reached. Although there was a period when the prevalent opinion was that a hydroxyl radical is formed in that reaction[5], lately there has been much discussion on the actual product[6], some authors favoring the formation of either an Fe(II)-hydroperoxo complex[7] or an Fe(IV) species[8] instead. Although recently reported kinetic data on the Fe(III) + H_2O_2 reaction in acid solution strongly suggest that it follows a hydroxyl-mediated chain mechanism[9], the experimental conditions in that study were far from those found in biological systems.

On the other hand, the cytochromes are a family of proteins involved in the respiratory chain of all aerobic organisms. One of its members, cytochrome *c*, is a small-size water-soluble protein found in the mitochondria, whose Fe-containing heme group oscillates between the Fe(III) and Fe(II) states as this freely-diffusible molecule mediates in the flow of electrons from cytochrome *c* reductase to cytochrome *c* oxidase, two large-size enzymes located in the inner mitochondrial membrane of eukaryotic cells. The mitochondria are thought to be the source of most of the hydroxyl radicals and other oxygen reactive species formed in aerobes[10]. Those species might be involved in processes such as oxidative stress, apoptosis and aging[11]. The decline of the efficiency of mitochondria as the source of energy for the cell requirements associated with senescence might also have a radical origin[12].

One of the possible biological sources of hydroxyl radicals is the cytochrome *c* + hydrogen peroxide reaction[13–15]. The oxidation of the reduced form of cytochrome *c* with hydrogen peroxide has been reported to be of first order in H_2O_2 and it is inhibited by benzoate ion, a hydroxyl radical scavenger, thus suggesting the formation of this radical as an intermediate[16]. This reaction is of interest because it is believed to play a key

role in the oxidation of mitochondrial phospholipids initiating apoptosis[17]. Hydrogen peroxide is known to cause destruction of cytochrome *c* as evidenced by decreased absorbance in the Soret band of its optical spectrum and the appearance of a new EPR signal with $g = 4.3$, both features being indicative of significant disturbance in the heme environment and suggesting decomposition of the tertiary structure of the protein[18]. Now, a kinetic study on the cytochrome *c* + hydrogen peroxide reaction under near-physiological pH conditions is presented.

EXPERIMENTAL

Materials and Methods

The solvent was water previously purified by deionization, distillation and circulation through a three-column Millipore system ($\kappa \approx 10^{-7}\ \Omega^{-1}\ cm^{-1}$). Horse-heart cytochrome *c* (Type III), superoxide dismutase (from bovine erythrocytes), D-mannitol and acrylamide were supplied by Sigma; H_2O_2 (30% additive-free aqueous solution), K_2CrO_4 and $Na_2WO_4 \cdot 2H_2O$ by Fluka; $Na_2MoO_4 \cdot 2H_2O$ by Riedel–de Haën; and KH_2PO_4, $K_2HPO_4 \cdot 3H_2O$, KCl, KBr, KNO_3, $NaHCO_2$, $ZnSO_4 \cdot 7H_2O$, $NaVO_3$, $K_3[Fe(CN)_6]$ and $K_4[Fe(CN)_6] \cdot 3H_2O$ by Merck. The initial concentrations of H_2O_2 were confirmed by permanganate titration in the presence of sulfuric acid. The pH measurements were made with a Metrohm 605 pH-meter provided with a glass-calomel combined electrode. The UV-VIS spectra were recorded with a Shimadzu UV-160 A double-beam spectrophotometer, using quartz cells (pathlength 1 cm). The kinetic runs were followed with a Varian Cary 219 spectrophotometer, measuring the decays of either the oxidized form of the protein (cyt-Fe(III)) at 394 nm or the reduced form (cyt-Fe(II)) at 550 nm, and the formation of $[Fe(CN)_6]^{3-}$ at 420 nm. All the kinetic experiments were duplicated, the total number of experiments was 421, and the typical random error of the kinetic data was ±2%.

Determination of Kinetic Data

The kinetic experiments were carried out under pseudo-first-order conditions (large excess of H_2O_2 with respect to cytochrome *c*). The kinetic plots showed slight deviations from the expected pseudo-first-order behavior at the beginning of the reaction, but in most cases a linear stretch was reached shortly after (Fig. 1). The experimental second-order rate constants (k_{exp}) were obtained from a fit of the absorbance-time data for that linear stretch to the equation

$$\ln (A_t - A_\infty) = \ln (A_0 - A_\infty) - k_{exp} [H_2O]_0\, t \qquad (2)$$

where A_0, A_t and A_∞ are the absorbances at the beginning of the reaction, at time *t* and at the end of the reaction, respectively. In other cases, the kinetic plots followed an autocatalytic pattern. The rate values corresponding to different times during the course of the reaction were then obtained by an approximate derivation method by means of the equation

$$v_t = -\frac{1}{\varepsilon l}\frac{\mathrm{d}A_t}{\mathrm{d}t} \approx -\frac{1}{\varepsilon l}\frac{\Delta A_t}{\Delta t} \qquad (3)$$

applied at short time intervals (Δt = 1 min), where $\varepsilon = 3.65 \times 10^4$ l mol^{-1} cm^{-1} is the molar absorption coefficient of oxidized cytochrome *c* at 394 nm and l = 1 cm is the optical pathlength. In these autocatalytic experiments, as well as in some of the non-autocatalytic ones, the kinetic data were obtained by application of the initial-rate method, through a nonlinear least-square fit of the absorbance–time data for the first stretch of each kinetic plot to the third-degree polynomial

$$\ln (A_t - A_\infty) = \ln (A_0 - A_\infty) + bt + ct^2 + dt^3 \qquad (4)$$

where parameters *c* and *d* account for the deviation of the kinetic plot with respect to the pseudo-first-order linear behavior, the initial rate being obtained as $v_0 = -b$ [cytochrome *c*]$_0$.

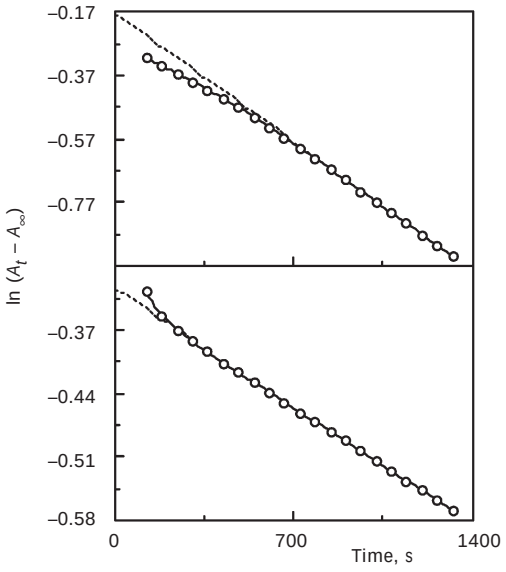

FIG. 1

Pseudo-first-order plots for the reaction of cytochrome *c* (1.60×10^{-5} mol l^{-1}) with H_2O_2 (1.88×10^{-3} mol l^{-1}) in the presence of phosphate buffer ([KH_2PO_4] + [K_2HPO_4] = 0.144 mol l^{-1}) at pH 5.66 (bottom) and 7.18 (top), ionic strength 2.10 mol l^{-1} (KCl) and 25.0 °C. The dashed lines correspond to perfect pseudo-first-order kinetics

RESULTS

UV-VIS Spectra

The spectrum recorded for the oxidized form of cytochrome *c* showed five absorption bands in the region 279–695 nm (Fig. 2, top). The corresponding ε values were consistent with those reported in the literature (deviation 2–9%)[19,20]. The presence of the weak band at 695 nm has been related to a higher reactivity of oxidized cytochrome *c* toward reducing agents such as ascorbate ion[21,22].

Upon stirring, the yellow aqueous solution containing the mixture of products from the cytochrome *c* + H_2O_2 reaction formed considerably more foam than the red-brown initial reactants solution, indicating that the oxidative-degradation products had a higher surfactant character than the native protein. After the reaction with a large excess of H_2O_2, both in the absence and in the presence of K_2CrO_4, the spectra showed shapeless profiles (Fig. 2, bottom), with the absorbance continuously decreasing with in-

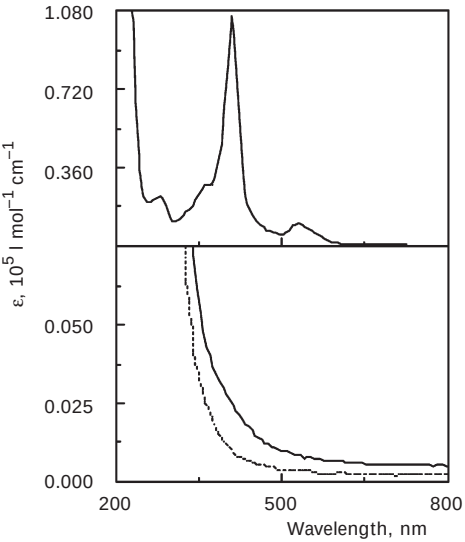

FIG. 2
UV-VIS spectra at 25.0 °C. Top: of cytochrome *c* (oxidized form) in the presence of KH_2PO_4–K_2HPO_4 (7.20×10^{-2} mol l^{-1} both) buffer at pH 6.79. Bottom: of the products obtained after 27 h from the reaction of cytochrome *c* (3.99×10^{-5} mol l^{-1}) with H_2O_2 (0.294 mol l^{-1}) in the presence of KH_2PO_4–K_2HPO_4 (6.00×10^{-2} mol l^{-1} both) buffer at pH 6.70 with [K_2CrO_4] = 0 (solid line) and 1.28×10^{-5} mol l^{-1} (dashed line)

creasing wavelength, in accordance with the behavior expected from Rayleigh's law for light scattering by colloidal particles[23], indicating that the heme prosthetic group of the protein (the one responsible for the light absorption) had been destroyed. At all wavelengths, the optical density for the final product mixture from the reaction in the absence of chromate (τ) was higher than that corresponding to the reaction in the presence of chromate (τ'), the measurements at 73 wavelengths in the range 380–800 nm yielding the ratio $\tau/\tau' = 2.38 \pm 0.19$. Since, for a given wavelength, the optical density associated with light scattering by colloidal particles is directly proportional to the second power of the particle polarizability[24], the ratio calculated for the corresponding polarizabilities was $\alpha/\alpha' = 1.54 \pm 0.06$. Given that the polarizability is proportional to the size of the colloidal particle, the decrease in the resulting particle polarizability when chromate was added to the reaction mixture seems to indicate that addition of K_2CrO_4 enhanced the oxidative degradation of cytochrome *c* caused by H_2O_2.

Kinetic Data

The oxidative degradation of the protein occurred at all concentrations of H_2O_2 (Fig. 3), with no critical peroxide concentration required to start the

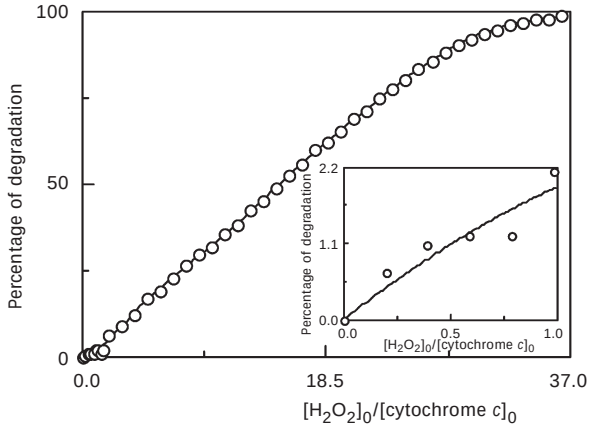

FIG. 3

Dependence of the percentage of protein degradation on the peroxide/protein initial concentration ratio measured 23 h after the beginning of the reaction of cytochrome *c* (7.99×10^{-6} mol l^{-1}) with H_2O_2 (variable concentration) in the presence of KH_2PO_4–K_2HPO_4 (7.20×10^{-2} mol l^{-1} both) buffer at pH 6.79 ± 0.01 and 25.0 °C. Inset: detail showing the dependence at low peroxide/protein ratios

degradation process, since a partial degradation took place even at low peroxide/protein ratios (Fig. 3, inset). The log v_0 vs log [cytochrome c]$_0$ linear plot (Fig. 4) yielded a value of 1.01 ± 0.01 for the kinetic order of cytochrome c. The log v_0 vs log [H_2O_2] linear plot (Fig. 4, inset) yielded a value of 1.05 ± 0.01 for the kinetic order of H_2O_2. Thus, the reaction followed the rate law

$$v = k_{exp}\,[\text{cytochrome } c][H_2O_2]. \qquad (5)$$

The k_{exp} vs pH plot showed base catalysis, and the experimental data could be fitted by nonlinear-least squares to the equation (Fig. 5)

$$k_{exp} = \frac{A + B[H^+]}{1 + C[H^+]} \qquad (6)$$

with A = 0.38 ± 0.04 l mol^{-1} s^{-1}, B = (2.9 ± 1.1) × 10^5 l^2 mol^{-2} s^{-1} and C = (4.2 ± 1.2) × 10^6 l mol^{-1} (at ionic strength 2.10 mol l^{-1} and 25.0 °C).

Increasing the concentrations of buffer (phosphate), KNO_3 or $NaHCO_2$ resulted in a slight increase in k_{exp} at low concentrations followed by a decrease at higher concentrations, but addition of KCl provoked a decrease in

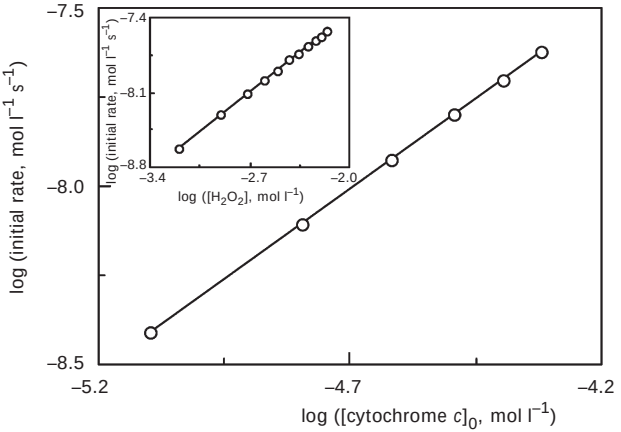

FIG. 4

Double-logarithm plots for the dependences of the initial rate of the cytochrome c + H_2O_2 reaction on the concentrations of cytochrome c (main plot: [H_2O_2] = 1.88 × 10^{-3} mol l^{-1}) and H_2O_2 (inset: [cytochrome c]$_0$ = 1.60 × 10^{-5} mol l^{-1}) in the presence of KH_2PO_4–K_2HPO_4 (7.20 × 10^{-2} mol l^{-1} both) buffer at pH 6.79 ± 0.01 and 25.0 °C

k_{exp} at all concentrations (Fig. 5, insets). Addition of KBr in a low concentration resulted in autocatalytic rate versus time plots (Fig. 6), and in a high concentration the formation of an intermediate absorbing light at 394 nm was observed at the beginning of the kinetic runs (Fig. 6, inset).

The reaction was inhibited by addition of some oxidants (Fig. 7). At low concentrations, the efficiency as inhibiting agents increased in the order $K_3[Fe(CN)_6]$ < Na_2WO_4 < Na_2MoO_4 < $NaVO_3$. At high concentrations, an increase in the concentration of $NaVO_3$ resulted in an increase in k_{exp}. On addition of Na_2WO_4, Na_2MoO_4 or $NaVO_3$ the rate versus time plots showed autocatalytic profiles (Fig. 8). Unlike the other oxidants tested, addition of K_2CrO_4 in a low concentration resulted in a slight increase in k_{exp} (Fig. 8, inset).

Two hydroxyl-radical scavengers (acrylamide[25] and D-mannitol[26]) and two superoxide-ion scavengers (zinc ion and superoxide dismutase[27]) were tested. Acrylamide in a low concentration (up to 1.77×10^{-2} mol l^{-1}) did not appreciably affect the initial rate, but the addition in a high concentration (0.36–1.80 mol l^{-1}) resulted in an increase in k_{exp} (Table I), the rate versus time plots becoming slightly autocatalytic. D-Mannitol provoked

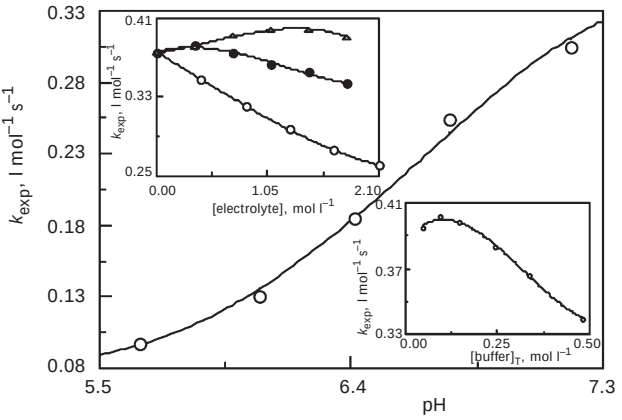

FIG. 5

Experimental rate constants for the reaction of cytochrome *c* (1.60×10^{-5} mol l^{-1}) with H_2O_2 (1.88×10^{-3} mol l^{-1}) at 25.0 °C. Main plot: dependence on pH at $[KH_2PO_4] + [K_2HPO_4] = 0.144$ mol l^{-1} and ionic strength 2.10 mol l^{-1} (KCl); the solid line represents the fit of the experimental data to Eq. (*6*). Left inset: dependence on the concentration of electrolyte at $[KH_2PO_4] = [K_2HPO_4] = 7.20 \times 10^{-2}$ mol l^{-1} and pH 6.79; electrolytes: KCl (○), KNO_3 (●) and $NaHCO_2$ (△). Right inset: dependence on the total concentration of buffer ($[KH_2PO_4] = [K_2HPO_4] = [buffer]_T/2$) at pH 6.90. Increasing either electrolyte or buffer concentration resulted in a decrease in pH. The rate constants are corrected to constant pH

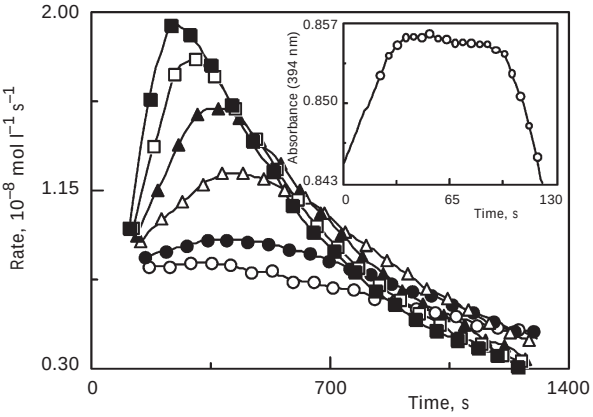

FIG. 6

Effect of KBr on the rate vs time plots for the reaction of cytochrome *c* (1.60×10^{-5} mol l^{-1}) with H_2O_2 (1.88×10^{-3} mol l^{-1}) in the presence of KH_2PO_4–K_2HPO_4 (7.20×10^{-2} mol l^{-1} both) buffer at 25.0 °C. [KBr] = 0 (○, pH 6.79), 0.036 (●, pH 6.74), 0.072 (△, pH 6.72), 0.108 (▲, pH 6.71), 0.144 (□, pH 6.69) and 0.180 (■, pH 6.67) mol l^{-1}. Inset: absorbance at 394 nm vs time plot at [KBr] = 0.360 mol l^{-1} and pH 6.61, the other conditions remaining the same

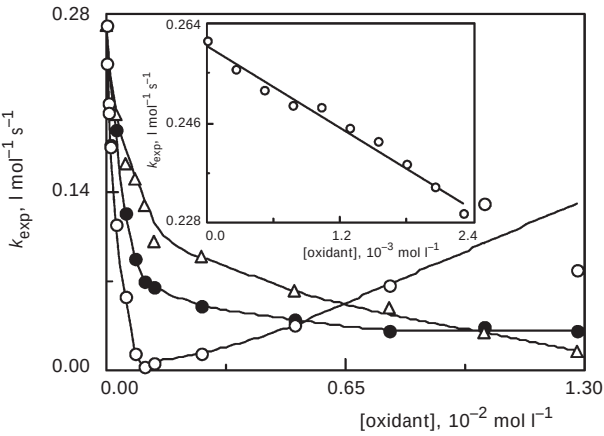

FIG. 7

Dependence of the experimental rate constant on the concentration of oxidant for the reaction of cytochrome *c* (1.60×10^{-5} mol l^{-1}) with H_2O_2 (1.88×10^{-3} mol l^{-1}) in the presence of KH_2PO_4–K_2HPO_4 (7.20×10^{-2} mol l^{-1} both) buffer at pH 6.79 ± 0.01 and 25.0 °C. Oxidants: $NaVO_3$ (○), Na_2MoO_4 (●) and Na_2WO_4 (△). Addition of Na_2WO_4 resulted in an increase in pH (range 6.79–6.98), the rate constants are corrected to constant pH (6.79). Inset: effect of $K_3[Fe(CN)_6]$ under the same conditions

TABLE I
Experimental rate constants of the cytochrome *c* + H_2O_2 reaction at various concentrations of acrylamide[a]

[Acrylamide], mol l^{-1}	k_{exp}, l mol^{-1} s^{-1}
0.000	0.278 ± 0.002[b]
0.004	0.291 ± 0.001[b]
0.007	0.282 ± 0.001[b]
0.011	0.271 ± 0.002[b]
0.014	0.289 ± 0.007[b]
0.018	0.271 ± 0.004[b]
0.360	0.304 ± 0.011[c]
0.720	0.354 ± 0.004[c]
1.080	0.399 ± 0.015[c]
1.440	0.542 ± 0.006[c]
1.800	0.839 ± 0.038[c]

[a] [cytochrome *c*]$_0$ = 1.60 × 10^{-5} mol l^{-1}, [H_2O_2] = 1.88 × 10^{-3} mol l^{-1}, [KH_2PO_4] = [K_2HPO_4] = 7.20 × 10^{-2} mol l^{-1}, 25.0 °C. [b] Rate constants determined at constant pH (6.79). [c] Addition of acrylamide in high concentrations resulted in a pH increase (range 6.79–6.98); the rate constants are corrected to constant pH (6.79).

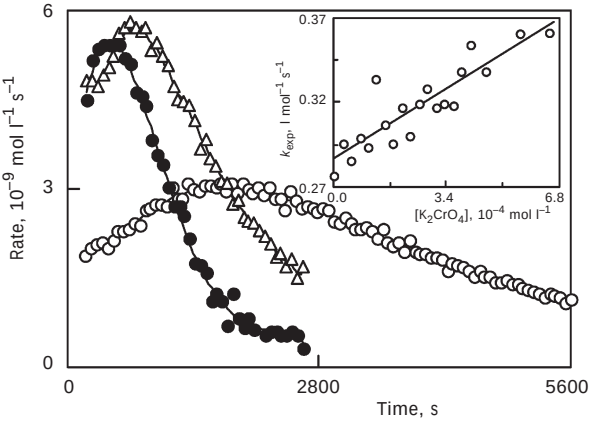

FIG. 8
Effect of several oxidants on the rate vs time plots for the reaction of cytochrome *c* (1.60 × 10^{-5} mol l^{-1}) with H_2O_2 (1.88 × 10^{-3} mol l^{-1}) in the presence of KH_2PO_4–K_2HPO_4 (7.20 × 10^{-2} mol l^{-1} both) buffer at 25.0 °C. Oxidants: Na_2MoO_4 (2.56 × 10^{-3} mol l^{-1}, pH 6.79, ○), $NaVO_3$ (2.56 × 10^{-4} mol l^{-1}, pH 6.79, ●) and Na_2WO_4 (2.56 × 10^{-3} mol l^{-1}, pH 6.83, △). Inset: dependence of the experimental rate constant on the concentration of K_2CrO_4 for the reaction of cytochrome *c* (1.60 × 10^{-5} mol l^{-1}) with H_2O_2 (6.26 × 10^{-4} mol l^{-1}) in the presence of KH_2PO_4–K_2HPO_4 (7.20 × 10^{-2} mol l^{-1} both) buffer at pH 6.79 ± 0.01 and 25.0 °C

a decrease of k_{exp}, but it was not a very efficient inhibitor since a high concentration of D-mannitol (0.384 mol l^{-1}) caused only a 10% inhibition (Fig. 9). This slight inhibition contrasts with the stronger inhibition caused by the same antioxidant on the reaction of cytochrome *c* with an organic cyclic peroxide (76%)[28]. Addition of either zinc ion in low concentration (up to 5.47×10^{-5} mol l^{-1}) or superoxide dismutase (up to 4.68×10^{-2} g l^{-1}) did not appreciably affect the initial rate.

The k_{exp} versus temperature data in the range 10–50 °C fulfilled both the Arrhenius and Eyring equations (Fig. 9, inset), yielding the apparent (pH-dependent) activation parameters E_a = 46 ± 2 kJ mol^{-1}, $\Delta H^{o}_{\neq}$ = 43 ± 2 kJ mol^{-1} and $\Delta S^{o}_{\neq}$ = –111 ± 5 J K^{-1} mol^{-1}.

Mixtures of cyt-Fe(III) and potassium hexacyanoferrate(II) in the presence of phosphate buffer were incubated in a thermostated bath at 25.0 °C. After 15 min of incubation, H_2O_2 was added and the decrease in absorbance at 550 nm was followed spectrophotometrically. The initial absorbance increased as the initial concentration of $[Fe(CN)_6]^{4-}$ increased (Fig. 10, top), as a result of the formation of cyt-Fe(II)[29,30]. The second-order rate constant for the reaction between cyt-Fe(II) and H_2O_2 (k'_{exp}) decreased as the initial concentration of $[Fe(CN)_6]^{4-}$ increased, according to the law

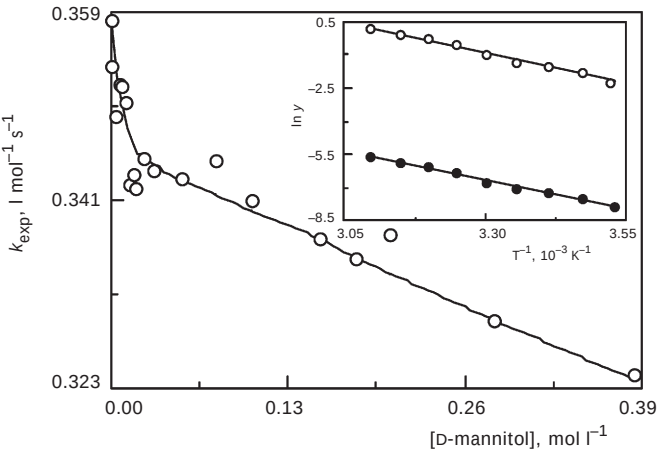

FIG. 9

Experimental rate constants for the reaction of cytochrome *c* (1.60×10^{-5} mol l^{-1}) with H_2O_2 (1.88×10^{-3} mol l^{-1}) in the presence of KH_2PO_4–K_2HPO_4 (7.20×10^{-2} mol l^{-1} both) buffer at pH 6.79 ± 0.01. Main plot: dependence on the concentration of D-mannitol at 25.0 °C; increasing the additive concentration resulted in a decrease in pH (range 6.79–6.70). The rate constants are corrected to constant pH (6.79). Inset: Arrhenius (○, $y = k_{exp}$) and Eyring (●, $y = k_{exp}/T$) plots

$$k'_{exp} = \frac{k}{1 + k'[Fe(CN)_6^{4-}]_0} \qquad (7)$$

indicating that $[Fe(CN)_6]^{4-}$ acted as an inhibitor for that reaction. From the intercept of the linear $1/k'_{exp}$ vs $[Fe(CN)_6^{4-}]_0$ plot (Fig. 10, bottom) the second-order rate constant for the oxidation of cyt-Fe(II) with H_2O_2 in the absence of inhibitor was evaluated to be 47 ± 3 l mol^{-1} s^{-1} (at ionic strength 0.288 mol l^{-1}, pH 6.79 and 25.0 °C). This value is of the same order of magnitude as that reported by some authors (13 l mol^{-1} s^{-1})[31], but it is much lower than that reported by others (8×10^3 l mol^{-1} s^{-1})[32]. The large discrepancy with the latter value might be explained by the fact that it was not determined by a direct measurement of the decay of cyt-Fe(II) at 550 nm, but by an indirect method in which the coupled oxidations of cyt-Fe(II) and dihydroriboflavin with H_2O_2 were studied together, and the kinetic data were obtained by following the oxidation of dihydroriboflavin at 445 nm. The large value of the rate constant obtained by this method might indi-

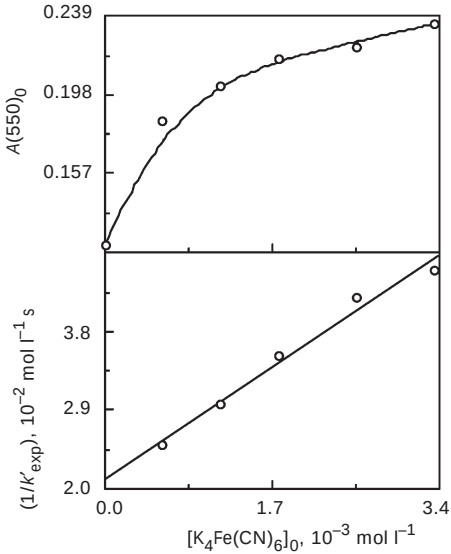

FIG. 10

Dependences of the initial absorbance at 550 nm (top) and of the reciprocal of the experimental rate constant for the oxidation of reduced cytochrome *c* with hydrogen peroxide (bottom) on the initial concentration of potassium hexacyanoferrate(II). [cytochrome *c*]$_0$ = 1.60×10^{-5} mol l^{-1}, $[H_2O_2] = 6.26 \times 10^{-4}$ mol l^{-1}, $[KH_2PO_4] = [K_2HPO_4] = 7.20 \times 10^{-2}$ mol l^{-1}, pH 6.79 ± 0.01, 25.0 °C

cate that the hydroxyl radicals formed in the cyt-Fe(II) + H_2O_2 reaction were engaged in a chain reaction leading to oxidation of dihydroriboflavin, so that the rate of decomposition of the latter was much higher than (and not equal to) the rate of the cyt-Fe(II) + H_2O_2 reaction (considered as the rate determining step). On the other hand, the value now obtained is very similar to the rate constant reported for a closely related reaction, the oxidation of $[Fe(H_2O)_6]^{2+}$ with H_2O_2 (58 l mol^{-1} s^{-1})[33].

Periodical scannings of the UV-VIS spectra for the reaction in the absence of hexacyanoferrate(II) ion (Fig. 11, bottom) showed a fast decay of the peaks at both 409 nm (Soret band) and 532 nm, with a well-defined isosbestic point at 332 nm. On the contrary, the periodical scannings in the presence of that ion (Fig. 11, top) showed in the initial stretch of the reaction a buildup of the first peak, indicating the formation of hexacyanoferrate(III) ion, whereas the second peak remained almost unaltered. The buildup of hexacyanoferrate(III) ion could be followed at 420 nm, and the kinetic plots at that wavelength corresponding to the reaction mixtures $K_4[Fe(CN)_6]$ + H_2O_2 and cytochrome *c* + H_2O_2, as well as to the combined

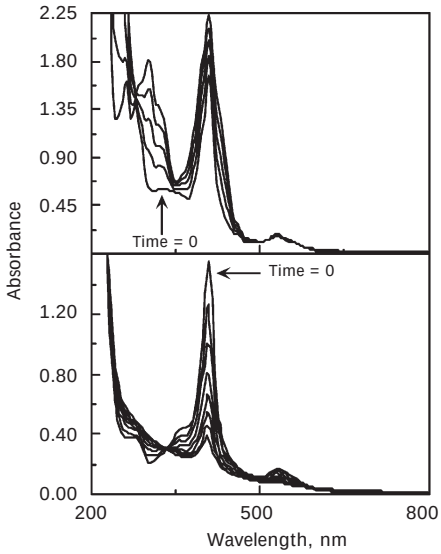

FIG. 11
Periodical scannings at 5 min intervals for the reaction of cytochrome *c* (1.60×10^{-5} mol l^{-1}) with H_2O_2 (1.96×10^{-3} mol l^{-1}) in the presence of KH_2PO_4–K_2HPO_4 (7.20×10^{-2} mol l^{-1} both) buffer at pH 6.79 ± 0.01 and 25.0 °C. $[K_4Fe(CN)_6]_0$ = 0 (bottom) and 9.88×10^{-4} mol l^{-1} (top)

reaction mixture $K_4[Fe(CN)_6]$ + cytochrome *c* + H_2O_2, are shown in Fig. 12. The first plot shows the formation of hexacyanoferrate(III) ion through the direct reaction of $[Fe(CN)_6]^{4-}$ with H_2O_2. The second plot shows the decay of cytochrome *c* at 420 nm through its reaction with H_2O_2. The third plot shows first the formation of hexacyanoferrate(III) ion and then the decay of cytochrome *c* corresponding to the combined reaction mixture, with an abrupt change of slope after the maximum. Addition of cytochrome *c* provoked a sharp increase in the initial rate of formation of hexacyanoferrate(III) ion. Thus, from the data in Fig. 12 it follows that cytochrome *c* acted as a catalyst for the $[Fe(CN)_6]^{4-}$ + H_2O_2 reaction, and also that $[Fe(CN)_6]^{4-}$ acted as a strong inhibitor of the cyt-Fe(III) + H_2O_2 reaction. Due to the mutual interference provoked at 420 nm by the decay of cyt-Fe(III) and the buildup of $[Fe(CN)_6]^{3-}$, only lower limits for the catalysis produced by cytochrome *c* (≥343%) and for the inhibition produced by $[Fe(CN)_6]^{4-}$ (≥85%) were obtained (Table II). That inhibition was attributable to the reduced form of the additive, $[Fe(CN)_6]^{4-}$, rather than to its oxidized form, $[Fe(CN)_6]^{3-}$, since an identical concentration of the latter would produce an inhibition of the cyt-Fe(III) + H_2O_2 reaction of only 5% (Fig. 7, inset). Thus, $[Fe(CN)_6]^{4-}$ was a much more efficient inhibitor of that reaction than $[Fe(CN)_6]^{3-}$.

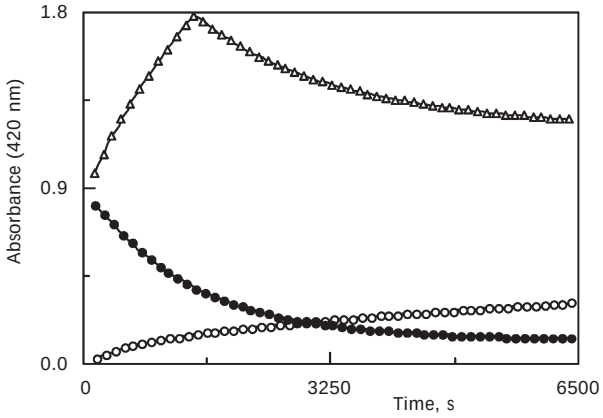

FIG. 12

Absorbance at 420 nm vs time plots for the reactions of cytochrome *c* and hexacyanoferrate(II) ion with H_2O_2 (1.88×10^{-3} mol l^{-1}) in the presence of KH_2PO_4–K_2HPO_4 (7.20×10^{-2} mol l^{-1} both) buffer at pH 6.79 ± 0.01 and 25.0 °C. For ○: [cytochrome *c*]$_0$ = 0 and $[K_4Fe(CN)_6]_0$ = 9.88×10^{-4} mol l^{-1}; for ●: [cytochrome *c*]$_0$ = 1.60×10^{-5} mol l^{-1} and $[K_4Fe(CN)_6]_0$ = 0; for △: [cytochrome *c*]$_0$ = 1.60×10^{-5} mol l^{-1} and $[K_4Fe(CN)_6]_0$ = 9.88×10^{-4} mol l^{-1}

TABLE II
Experimental rate constants for cytochrome *c* + H_2O_2 reaction mixtures in the absence and presence of hexacyanoferrate(II) ion[a]

Reactants	Decay/Buildup	k_{exp}, l mol^{-1} s^{-1}
cyt-Fe(III) + H_2O_2[b]	decay of cyt-Fe(III)	0.293 ± 0.013[c,d]
cyt-Fe(III) + $[Fe(CN)_6]^{4-}$ + H_2O_2[b,e]	decay of cyt-Fe(III)[f]	0.261 ± 0.003[c,g]
cyt-Fe(III) + $[Fe(CN)_6]^{4-}$ + H_2O_2[b,e]	decay of cyt-Fe(III)[h]	0.044 ± 0.007[i]
$[Fe(CN)_6]^{4-}$ + H_2O_2[e]	buildup of $[Fe(CN)_6]^{3-}$	0.114 ± 0.004[j]
cyt-Fe(III) + $[Fe(CN)_6]^{4-}$ + H_2O_2[b,e]	buildup of $[Fe(CN)_6]^{3-}$	0.505 ± 0.032[j,k]

[a] $[H_2O_2] = 1.88 \times 10^{-3}$ mol l^{-1}, $[KH_2PO_4] = [K_2HPO_4] = 7.20 \times 10^{-2}$ mol l^{-1}, pH 6.79 ± 0.01, 25.0 °C. [b] $[\text{cyt-Fe(III)}]_0 = 1.60 \times 10^{-5}$ mol l^{-1}. [c] From a ln $(A_t - A_\infty) = a + bt + ct^2 + dt^3$ non-linear least-squares fit, $k_{exp} = -b/[H_2O_2]$. [d] Initial stretch of the reaction. [e] $[K_4Fe(CN)_6]_0 = 9.88 \times 10^{-4}$ mol l^{-1}. [f] In the presence of $[Fe(CN)_6]^{3-}$. [g] Stretch right after the maximum of A_{420}, taking t_{max} as $t = 0$, lower limit for k_{exp} (assuming total conversion of $[Fe(CN)_6]^{4-}$ into $[Fe(CN)_6]^{3-}$ at t_{max}), inhibition ≤ 11%. [h] In the presence of $[Fe(CN)_6]^{4-}$. [i] The fraction of cyt-Fe(III) reacted at t_{max} was calculated as $f = (A_0 - A_{max})/(A_0 - A_\infty)$, where both A_{max} and A_∞ were corrected to discount the absorbance due to $[Fe(CN)_6]^{3-}$ (ε_{420} = 1015 l mol^{-1} cm^{-1}); $k_{exp} = -(\ln(1 - f))/(t_{max}[H_2O_2])$ (average value for the period $t = 0$–t_{max}), upper limit for k_{exp} (assuming total conversion of $[Fe(CN)_6]^{4-}$ into $[Fe(CN)_6]^{3-}$ at t_{max}), inhibition ≥ 85%. [j] From a ln $(A_\infty - A_t) = a' + b't + c't^2 + d't^3$ nonlinear least-squares fit in the initial stretch of the reaction, $k_{exp} = -b'/[H_2O_2]$. [k] Lower limit for k_{exp} (assuming total inhibition of the cyt-Fe(III) decay), catalysis ≥ 343%.

DISCUSSION

Mechanism

According to the results found in this work, the mechanism that can be proposed for the reaction consists of the following steps.

$$\text{cyt-Fe}^{3+} + H_2O_2 \underset{}{\overset{K_1}{\rightleftharpoons}} \text{cyt-Fe}^{3+} - H_2O_2 \qquad (8)$$

$$\text{cyt-Fe}^{3+} - H_2O_2 \overset{K_2}{\rightleftharpoons} \text{cyt-FeOOH}^{2+} + H^+ \qquad (9)$$

$$\text{cyt-Fe}^{3+} - H_2O_2 \xrightarrow[\text{slow}]{k_3} \text{cyt-Fe}^{2+} + HO_2^{\bullet} + H^+ \qquad (10)$$

$$\text{cyt-FeOOH}^{2+} \xrightarrow[\text{slow}]{k_4} \text{cyt-Fe}^{2+} + \text{HO}_2^{\bullet} \qquad (11)$$

$$\text{cyt-Fe}^{2+} + \text{H}_2\text{O}_2 \xrightarrow{k_5} \text{cyt-Fe}^{3+} + \text{HO}^- + \text{HO}^{\bullet} \qquad (12)$$

$$\text{cyt-Fe}^{3+} + \text{HO}^{\bullet} \xrightarrow{k_6} \text{oxidative-degradation products} \qquad (13)$$

$$\text{HO}_2^{\bullet} \underset{}{\overset{K_7}{\rightleftharpoons}} \text{H}^+ + \text{O}_2^{\bullet -} \qquad (14)$$

$$\text{HO}_2^{\bullet} + \text{O}_2^{\bullet -} \xrightarrow{k_8} \text{HO}_2^- + \text{O}_2 \qquad (15)$$

The first step (Eq. (*8*)) corresponds to the formation of a complex between the two reactants. This complex suffers a partial deprotonation in Eq. (*9*), so that the reaction takes place through two different pathways, each of them with its own rate-determining step, corresponding to the one-electron reduction of the iron atom of the protein from Fe(III) to Fe(II) whereas H_2O_2 is oxidized to an $HO_2^{\bullet}$ radical (Eqs (*10*) and (*11*)). In the following fast reactions, cyt-Fe(II) is reoxidized with H_2O_2 to cyt-Fe(III) with the formation of a hydroxyl radical (Eq. (*12*)), then the latter attacks the heme prosthetic group of the protein yielding oxidative-degradation products (Eq. (*13*)). Although hydroxyl radicals may also be involved in the reduction of cyt-Fe(III) to cyt-Fe(II) with the intermediation of a tunnelling effect[34], this alternative reaction would not affect the rate law, because of its taking place after the rate determining steps (Eqs (*10*) and (*11*)). The $HO_2^{\bullet}$ radical formed is in equilibrium with the superoxide radical (Eq. (*14*)). Finally, the latter two species are destroyed in a dismutation step (Eq. (*15*)), facilitated by the oxidizing character of the acid form of this intermediate ($HO_2^{\bullet}$) due to its low electron density, and the reducing character of the basic form ($O_2^{\bullet -}$) due to its high electron density. Although superoxide ions are known to reduce cyt-Fe(III)[35–38], the failure of the superoxide-radical scavengers, zinc ion and superoxide dismutase, to inhibit the reaction suggests that the final destiny of superoxide ions was to disappear by dismutation rather than by transferring their electrons in excess to other protein molecules. It is thus probable that most of the $HO_2^{\bullet}$ and $O_2^{\bullet -}$ radi-

cals generated in Eqs (*10*), (*11*) and (*14*) could not escape from the protein lattice belonging to the cyt-Fe(II) molecule on the surface of which they were formed to attack other cyt-Fe(III) molecules. Since the peptide chain of cytochrome *c* is known to possess many lysine fragments with the ε-amino groups in their protonated forms[39], one of them might electrostatically bind the first superoxide ion formed (anionic ligands are known to specifically bind to cytochrome *c*)[40] until a second superoxide ion is generated on the same protein molecule and dismutation is possible (Eq. (*15*)). Moreover, the protonated ε-amino group of lysine might act as a proton donor for one of the superoxide ions, thus facilitating the dismutation process.

The use of UV-VIS difference spectroscopy, by subtracting the spectrum of the native protein from that of the reaction mixture, has allowed to detect the formation of an intermediate at low peroxide/protein ratios ($[H_2O_2]_0$/[cytochrome *c*]$_o \approx 1$). The difference spectrum shows an absorption peak at 402 nm and an absorption valley at 417 nm (Fig. 13, bottom). The

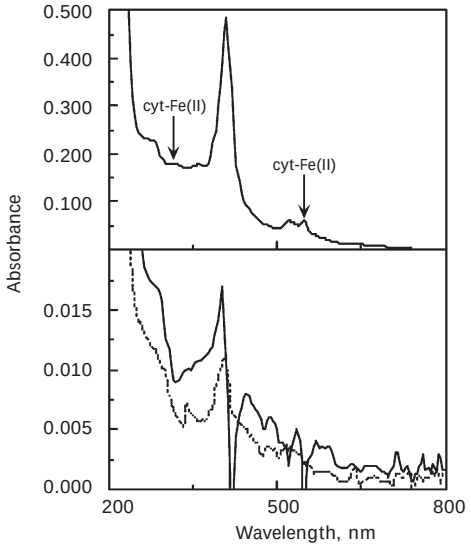

FIG. 13

UV-VIS spectra for the reaction of cytochrome *c* (7.99×10^{-6} mol l^{-1}) with H_2O_2 in the presence of KH_2PO_4–K_2HPO_4 (7.20×10^{-2} mol l^{-1} both) buffer at pH 6.79 ± 0.01 and 25.0 °C. Top: ordinary spectrum recorded 23 h after the beginning of the reaction with $[H_2O_2]_0 = 1.10 \times 10^{-4}$ mol l^{-1}, the arrows indicating the wavelengths corresponding to the intermediate cyt-Fe(II). Bottom: difference spectra recorded 12 min (dashed line) and 83 min (solid line) after the beginning of the reaction, the solutions contained in the spectrophotometer cells differing only in the concentration of $[H_2O_2]_0$ either 7.83×10^{-6} mol l^{-1} (main cell) or 0 (reference cell)

presence of this peak-valley couple is consistent with a 7-nm shift of the Soret band (located in the spectrum of the native protein at 409 nm) toward lower wavelengths, and might be indicative of the formation of a protein–peroxide intermediate complex (Eqs (*8*) and (*9*)). The difference spectrum also showed a second absorption valley at 549 nm, indicating that a small fraction of the commercial protein preparation was in the reduced form, and that it was oxidized after addition of H_2O_2, thus confirming Eq. (*12*). Moreover, the use of UV-VIS ordinary spectroscopy has allowed to detect the formation of a second intermediate at intermediary peroxide/protein ratios ($[H_2O_2]_0$/[cytochrome $c]_0$ = 14), the spectrum showing a shoulder at 300–320 nm and a peak at 549 nm (Fig. 13, top), both consistent with the formation of cyt-Fe(II) as an intermediate (Eqs (*10*) and (*11*))[19].

Although there has been a certain controversy on the nature of the oxidizing species formed in the reactions of Fe(II) complexes with H_2O_2, the results found in the present work are more consistent with the hypothesis that, at least in the case of the cyt-Fe(II) + H_2O_2 reaction (Eq. (*12*)), the oxidizing species formed is a hydroxyl radical than with the alternative hypotheses that it is either an Fe(II)-hydroperoxo complex (cyt-$FeOOH^+$) or an Fe(IV) complex (cyt-FeO^{2+}). Since in cytochrome *c* the six coordination sites of the iron atom are used to bind it to the rest of the protein, four bonds with nitrogen atoms belonging to the heme prosthetic group and the other two bonds with His 18 and Met 80 of the peptide chain[41], the iron atom in the hypothetic cyt-$FeOOH^+$ or cyt-FeO^{2+} complexes would still keep five bonds with the rest of the protein. Those complexes would thus lack the mobility required to explain the extensive oxidative degradation of the protein experimentally observed (Fig. 2, bottom). On the contrary, a degradation of cytochrome *c* similar to that observed in the present work has been reported to occur on its reaction with hydroxyl radicals generated by γ-radiolysis[42,43]. However, the involvement of either cyt-$FeOOH^+$ or cyt-FeO^{2+} as transient intermediates in the formation of hydroxyl radicals from cyt-Fe(II) + H_2O_2 cannot be discarded.

Interpretation of Kinetic Data

The finding of a well-defined isosbestic point for the reaction with a large excess of H_2O_2 with respect to cytochrome *c* (Fig. 11, bottom) indicated that, under those experimental conditions, all the intermediates involved in the mechanism were in concentrations low enough to apply the steady-state approximation. Application of the quasi-equilibrium approximation

to the steps given by Eqs (*8*) and (*9*), and of the steady-state approximation to the intermediates cyt-Fe(II) and $HO^{\bullet}$, leads to the rate law

$$v = \frac{K_1(K_2 k_4 + k_3[H^+])}{K_2 + [H^+]} [\text{cytochrome } c][H_2O_2] \qquad (16)$$

in agreement with Eqs (*5*) and (*6*) provided that $A = K_1k_4$, $B = K_1k_3/K_2$ and $C = 1/K_2$. From the experimental values of parameters *A*, *B* and *C*, the values of K_1k_3, K_1k_4, and K_2 were obtained. The value of k_5 was obtained in the present work from the experiments in the presence of $[Fe(CN)_6]^{4-}$ (see Results). The values of k_6, K_7 and k_8 have been obtained from the literature (Table III)[27,44]. From the value of equilibrium constant K_2 we obtain $pK_2 = 6.62 \pm 0.12$, a value much lower than that of $pK_a = 11.6$ for the dissociation of H_2O_2 (ref.[45]), which is consistent with the fact that coordination of the H_2O_2 molecule to a low electron-density site such as Fe(III) is expected to increase its acidity. Moreover, from the ratio $k_4/k_3 = 5.6$ it follows that the basic form of the cyt-Fe(III)–H_2O_2 complex reacted considerably faster than the acid form, which is also consistent with the fact that an increase in the electron density of the ligand bound to Fe(III) (HO_2^- vs H_2O_2) results in an increase in the reducing character of that ligand and explains the base catalysis shown in Fig. 5.

The finding that the phosphate buffer and the electrolytes KNO_3 and $NaHCO_2$ caused an increase in k_{exp} at low concentrations followed by a decrease at higher concentrations, whereas KCl caused a continued decrease

TABLE III
Equilibrium and rate constants for the elementary steps of the mechanism proposed for the cytochrome *c* + H_2O_2 reaction at 25.0 °C

Constant	Value	Source
K_1k_3	$(6.8 \pm 1.2) \times 10^{-2}$ l mol^{-1} s^{-1}	this work
K_1k_4	0.38 ± 0.041 l mol^{-1} s^{-1}	this work
K_2	$(2.4 \pm 0.7) \times 10^{-7}$ mol l^{-1}	this work
k_5	47 ± 3 l mol^{-1} s^{-1}	this work
k_6	$\geq 1.4 \times 10^{10}$ l mol^{-1} s^{-1}	ref.[44]
K_7	2.0×10^{-5} mol l^{-1}	ref.[27]
k_8	1.0×10^{8} l mol^{-1} s^{-1}	ref.[27]

of k_{exp} at all concentrations (Fig. 5, insets), is similar to the complex behavior toward electrolytes observed for the rate of other cytochrome *c* reactions, such as the oxidation of cyt-Fe(II) by O_2 in the presence of NaCl (increase followed by decrease) or $NaClO_4$ (continued increase)[46]. Moreover, the reduction potential of cyt-Fe(III) decreases by addition of a non-binding electrolyte (Tris-cacodylate buffer) and increases by addition of a binding electrolyte (NaCl)[47]. Thus, the increase in k_{exp} in the cytochrome *c* + H_2O_2 reaction might be an ionic-strength effect whereas the decrease in k_{exp} might be an anion-binding effect. This is consistent with the facts that Cl^- and phosphate ions are known to bind to cytochrome *c* (both oxidized and reduced forms)[40] and that the photoinduced reduction of cyt-Fe(III) in the presence of a hydroperoxide derivative of biphenyl was inhibited by salts, their activities being correlated to the electron-donating nature of the anions[48].

The fact that addition of HCO_2^- in a low concentration accelerated the oxidative degradation of cytochrome *c* by H_2O_2 contrasts with the inhibition caused by that ion in the degradation of folic acid by the cytochrome *c* + H_2O_2 reaction[49]. This suggests that HCO_2^- efficiently traps the hydroxyl radicals that escape from the protein crevice containing the heme functional group (the ones involved in the degradation of folic acid) but not those hydroxyl radicals reacting in situ with the pyrrole rings of the heme prosthetic group.

The singular effect of KBr, quite different from that of KCl, might be probably related to the higher reducing power of Br^- as compared with that of Cl^-, causing the oxidation of Br^- to HBrO by H_2O_2. Since this reaction does not take place at an appreciable rate at neutral pH [50], it might be catalyzed by the protein, the Fe(III) atom serving as a support for the coordination of the two reactants (Br^- and H_2O_2). The accumulation in the solution of the intermediate HBrO might explain the autocatalysis observed in the presence of Br^- (Fig. 6), as HBrO is known to react with cytochrome *c* with a very high rate constant[51].

The inhibition caused by the oxidants $[Fe(CN)_6]^{3-}$, WO_4^{2-}, MoO_4^{2-} and VO_3^- (Fig. 7) can be explained by the oxidation of the cyt-Fe(II) intermediate with those oxidants, thus preventing the formation of hydroxyl radicals from the reaction of cyt-Fe(II) with H_2O_2 (Eq. (*12*)). Hence, the existence of that inhibition effect by oxidants can be taken as a proof supporting the involvement of the reduced form of cytochrome *c* as an active intermediate in the oxidative-degradation reaction. The rate-enhancing effect observed at very high concentrations of VO_3^- might be a consequence of the forma-

tion of a strong oxidant, diperoxovanadate(V) (VO_5^-), as an intermediate from the $VO_3^- + H_2O_2$ reaction[52]. The autocatalytic profile of the rate versus time plots in the presence of three of those oxidants (Fig. 8) can be ascribed to the disappearance of the inhibitor as its one-electron reduced form accumulates in the solution. The failure of CrO_4^{2-} to inhibit the cyt-Fe(III) + H_2O_2 reaction is consistent with the standard one-electron reduction potentials for the systems cyt-Fe(III)/cyt-Fe(II) (+0.26 V)[53] and CrO_4^{2-}/CrO_4^{3-} (+0.10 V)[54]. However, CrO_4^{2-} does inhibit the Cu(II) + H_2O_2 reaction[55], despite the potential for the system Cu^{2+}/Cu^+ (+0.16 V)[56] is just a little lower than that for cyt-Fe(III)/cyt-Fe(II). The finding that CrO_4^{2-}, instead of inhibiting as other oxidants, actually enhances (although only slightly) the rate of the oxidative degradation of the protein by H_2O_2 (Figs 2, bottom, and 8, inset) can be explained by the formation of additional hydroxyl radicals from the $CrO_4^{2-} + H_2O_2$ parallel reaction, thus contributing to the protein degradation (Eq. (*13*))[57].

The failure of acrylamide to inhibit the oxidative degradation of cytochrome *c* by H_2O_2 and the finding that it actually accelerated the reaction at high concentrations (Table I) can be explained by the ability of acrylamide to covalently bind to proteins such as cytochrome *c* by reacting with the ε-amino group of lysine fragments[58]. The finding that the inhibition caused by the hydroxyl-radical scavenger D-mannitol (Fig. 9) was only minor might be caused by the fact that cyt-Fe(III) and $HO^\bullet$ react in situ (Eq. (*13*)) immediately after the formation of that radical in the protein heme-containing crevice (Eq. (*12*)). The much stronger inhibition caused by $[Fe(CN)_6]^{4-}$ is consistent with the report that its second-order rate constant at 25.0 °C when acting as a hydroxyl-radical scavenger (1.0×10^{10} l mol^{-1} s^{-1})[59] is higher than that corresponding to D-mannitol (2.5×10^9 l mol^{-1} s^{-1})[60], and also than those corresponding to other hydroxyl-radical scavengers such as formate ion (3.2×10^9 l mol^{-1} s^{-1})[61] or acrylamide (5.9×10^9 l mol^{-1} s^{-1})[62]. Moreover, since at physiological pH cytochrome *c* has a polycationic nature caused mainly by the protonation of the lysine side amino groups[39], the highly negative electrostatic charge of the ion $[Fe(CN)_6]^{4-}$ might enhance its scavenging effect for hydroxyl radicals situated in the surroundings of a cytochrome *c* molecule.

Biological Implications

Although it is likely that most of the hydroxyl radicals generated in the oxidative degradation of cytochrome *c* by H_2O_2 react in situ with the protein, some of those radicals might escape from the crevice containing the heme

prosthetic group. This hypothesis is supported by the reports that the cytochrome *c* + H_2O_2 reaction causes the degradation of folic acid[49], and that a heme-nonapeptide proteolytic fragment of cytochrome *c* mediates in the hydroxylation of aniline with H_2O_2 (ref.[63]), suggesting that some of the hydroxyl radicals, instead of reacting with the heme group, escape into the solution and react with other oxidizable molecules. Thus, the cytochrome *c* + H_2O_2 reaction, besides causing the oxidative degradation of the protein, might be involved in other physiological side effects caused by the escaping hydroxyl radicals (one of the strongest oxidants known[64]), such as mitochondria degeneration and cell aging.

REFERENCES

1. Sohal R. S., Weindruch R.: *Science* **1996**, *273*, 59.
2. Al-Ajlouni A. M., Espenson J. H., Bakac A.: *Inorg. Chem.* **1993**, 32, 3162.
3. Meggers E., Holland P. L., Tolman W. B., Romesberg F. E., Schultz P. G.: *J. Am. Chem. Soc.* **2000**, *122*, 10714.
4. Toyokuni S.: *Free Radical Biol. Med.* **1996**, *20*, 553.
5. Walling C., Partch R. E., Weil T.: *Proc. Natl. Acad. Sci. U.S.A.* **1975**, *72*, 140.
6. Goldstein S., Meyerstein D.: *Acc. Chem. Res.* **1999**, *32*, 547.
7. Sawyer D. T., Sobkowiak A., Matsushita T.: *Acc. Chem. Res.* **1996**, *29*, 409.
8. Rachmilovich-Calis S., Masarwa A., Meyerstein N., Meyerstein D.: *Eur. J. Inorg. Chem.* **2005**, 2875.
9. Perez-Benito J. F.: *J. Phys. Chem. A* **2004**, *108*, 4853.
10. Iwase H., Takatori T., Aono K., Iwadate K., Takahashi M., Nakajima M., Nagao M.: *Biochem. Biophys. Res. Commun.* **1995**, *216*, 483.
11. Kajiwara K., Ikeda K., Kuroi R., Hashimoto R., Tokumaru S., Kojo S.: *Cell. Mol. Life Sci.* **2001**, *58*, 485.
12. Lenaz G., Cavazzoni M., Genova M. L., D'Aurelio M., Pich M. M., Pallotti F., Formiggini G., Marchetti M., Castelli G. P., Bovina C.: *BioFactors* **1998**, *8*, 195.
13. Kownatzki E., Uhrich S., Bethke P.: *Agents Actions* **1991**, *34*, 393.
14. Chung N., Shah M. M., Grover T. A., Aust S. D.: *Arch. Biochem. Biophys.* **1993**, *306*, 70.
15. Villegas J. A., Mauk A. G., Vazquez-Duhalt R.: *Chem. Biol.* **2000**, *7*, 237.
16. Turrens J. F., McCord J. M.: *FEBS Lett.* **1988**, *227*, 43.
17. Gourion-Arsiquaud S., Chevance S., Bouyer P., Garnier L., Montillet J. L., Bondon A., Berthornieu C.: *Biochemistry* **2005**, *44*, 8652.
18. Kagan V. E., Borisenko G. G., Tyurina Y. Y., Tyurin V. A., Jiang J., Potapovich A. I., Kini V., Amoscato A. A., Fujii Y.: *Free Radical Biol. Med.* **2004**, *37*, 1963.
19. Margoliash E., Frohwirt N.: *Biochem. J.* **1959**, *71*, 570.
20. Greenwood C., Wilson M. T.: *Eur. J. Biochem.* **1971**, *22*, 5.
21. Wilson M. T., Greenwood C.: *Eur. J. Biochem.* **1971**, *22*, 11.
22. Mathews A. J., Brittain T.: *Biochem. J.* **1987**, *243*, 379.
23. Perez-Benito J. F., Arias C.: *J. Colloid Interface Sci.* **1992**, *152*, 70.
24. Barrow G. M.: *Physical Chemistry*, p. 803. McGraw–Hill, New York 1966.
25. Perez-Benito J. F.: *J. Inorg. Biochem.* **2004**, *98*, 430.

26. Itoh M., Nakamura M., Suzuki T., Kawai K., Horitsu H., Takamizawa K.: *J. Biochem.* **1995**, *117*, 780.
27. Sawyer D. T., Valentine J. S.: *Acc. Chem. Res.* **1981**, *14*, 393.
28. Konishi T., Matsugo S.: *Biochim. Biophys. Acta* **1988**, *967*, 267.
29. Brandt K. G., Parks P. C., Czerlinski G. H., Hess G. P.: *J. Biol. Chem.* **1966**, *241*, 4180.
30. Perez-Benito J. F., Arias C., Brillas E.: *Gazz. Chim. Ital.* **1991**, *121*, 139.
31. Di Paolo M. L., Scarpa M., Rigo A.: *J. Biochem. Biophys. Methods* **1994**, *28*, 205.
32. Xu F., Hultquist E. D.: *Biochem. Biophys. Res. Commun.* **1991**, *181*, 197.
33. Bakac A.: *Prog. Inorg. Chem.* **1995**, *43*, 267.
34. Van Leeuwen J. W., Raap A., Koppenol W. H., Nauta H.: *Biochim. Biophys. Acta* **1978**, *503*, 1.
35. Koppenol W. H., Van Buuren K. J. H., Butler J., Braams R.: *Biochim. Biophys. Acta* **1976**, *449*, 157.
36. Butler J., Koppenol W. H., Margoliash E.: *J. Biol. Chem.* **1982**, *257*, 10747.
37. Butler J., Hoey B. M.: *Biochim. Biophys. Acta* **1993**, *1161*, 73.
38. Mitsuta K., Hiramatsu M., Ohya-Nishiguchi H., Kamada H., Fujii K.: *Bull. Chem. Soc. Jpn.* **1994**, *67*, 529.
39. Koppenol W. H., Margoliash E.: *J. Biol. Chem.* **1982**, *257*, 4426.
40. Gopal D., Wilson G. S., Earl R. A., Cusanovich M. A.: *J. Biol. Chem.* **1988**, *263*, 11652.
41. Sivakolundu S. G., Mabrouk P. A.: *J. Biol. Inorg. Chem.* **2003**, *8*, 527.
42. Koppenol W. H., Butler J.: *Isr. J. Chem.* **1984**, *24*, 11.
43. Koppenol W. H.: *Free Radical Biol. Med.* **1985**, *1*, 281.
44. Nilsson K.: *Isr. J. Chem.* **1972**, *10*, 1011.
45. Coetzee J. F., Ritchie C. D.: *Solute–Solvent Interactions*, p. 20. Dekker, New York 1969.
46. Harrington J. P., Carrier T. L.: *Int. J. Biochem.* **1985**, *17*, 119.
47. Margalit R., Schejter A.: *Eur. J. Biochem.* **1973**, *32* , 492.
48. Matsugo S., Kayamori-Sato N., Konishi T.: *Photochem. Photobiol.* **1994**, *60*, 415.
49. Taher M. M., Lakshmaiah N.: *J. Inorg. Biochem.* **1987**, *31*, 133.
50. Perez-Benito J. F.: *Monatsh. Chem.* **2001**, *132*, 1477.
51. Prutz W. A., Kissner R., Nauser T., Koppenol W. H.: *Arch. Biochem. Biophys.* **2001**, *389*, 110.
52. Ogata Y., Tanaka K.: *Can. J. Chem.* **1982**, *60*, 848.
53. Lojou E., Luciano P., Nitsche S., Bianco P.: *Electrochim. Acta* **1999**, *44*, 3341.
54. Bard A. J.: *Encyclopedia of Electrochemistry of the Elements*, Vol. IX, Part B, p. 263. Marcel Dekker, New York 1986.
55. Perez-Benito J. F., Arias C.: *New J. Chem.* **1999**, *23*, 945.
56. Weast R. C.: *Handbook of Chemistry and Physics*, p. D-141. CRC Press, Cleveland 1977.
57. Perez-Benito J. F., Arias C.: *J. Phys. Chem. A* **1997**, *101*, 4726.
58. Geisthardt D., Kruppa J.: *Anal. Biochem.* **1987**, *160*, 184.
59. Elliot A. J., McCracken D. R., Buxton G. V., Wood N. D.: *J. Chem. Soc., Faraday Trans.* **1990**, *86*, 1539.
60. Zhao M. J., Jung L., Tanielian C., Mechin R.: *Free Radical Res.* **1994**, *20*, 345.
61. Motohashi N., Saito Y.: *Chem. Pharm. Bull.* **1993**, *41*, 1842.
62. Buxton G. V., Greenstock C. L., Helman W. P., Ross A. B.: *J. Phys. Chem. Ref. Data* **1988**, *17*, 513.
63. Rusvai E., Vegh M., Kramer M., Horvath I.: *Biochem. Pharmacol.* **1988**, *37*, 4574.
64. Li B., Gutierrez P. L., Blough N. V.: *Anal. Chem.* **1997**, *69*, 4295.